Delay analysis of Ethernet passive optical networks with gated service

Frank Aurzada,[1] Michael Scheutzow,[1] Martin Herzog,[2] Martin Maier,[2] and Martin Reisslein[3,*]

[1] *Department of Mathematics, Technical University Berlin, 10623 Berlin, Germany*

[2] *Institut National de la Recherche Scientifique (INRS), Montréal, QC, H5A 1K6, Canada*

[3] *Department of Electrical Eng., Arizona State Univ., Tempe, AZ 85287-5706, USA*

[*] *Corresponding author: reisslein@asu.edu*

We analyze the mean packet delay in an Ethernet passive optical network (EPON) with gated service. For an EPON with a single ONU, we derive (i) a closed form delay expression for reporting at the end of an upstream transmission, and (ii) a Markov chain based approach requiring the numerical solution of a system of equations for reporting at the beginning of an upstream transmission. Reporting at the beginning, which has not been previously examined in detail, achieves significantly smaller delays than reporting at the end of an upstream transmission for a small number of ONUs. Both of these analyses are fundamentally different from existing polling system analyses in that they consider the dependent switchover times of the EPON. We extend the analysis for reporting at the beginning of an upstream transmission to approximate the mean packet delay in an EPON with multiple ONUs and verify the accuracy of the analysis with simulations. Overall, our numerical results indicate that for utilizations up to around 75%, the mean packet delay is close to its minimum of four times the one-way propagation delay.

OCIS codes: 060.4250, 060.4259, 000.5490.

1. Introduction

Ethernet passive optical networks (EPONs) have received significant interest recently for providing cost-effective high-speed Internet access, see for instance [1–15]. An EPON connects several optical network units (ONUs) via a shared network, typically with a tree or bus topology, with the optical line terminal (OLT), which in turn connects to metro and wide area networks. In order to avoid collisions of the upstream ONU-to-OLT transmissions, the OLT arbitrates the access of the ONUs to the shared upstream network through a dynamic bandwidth allocation (DBA) mechanism. In general, the OLT issues transmission grants to the ONUs that are timed such that successive upstream transmissions arriving at the OLT are spaced by at least a standard defined guard time. Akin to a polling mechanism, the DBA is cyclical in that each ONU includes a REPORT message indicating the amount of newly generated upstream traffic in a granted upstream transmission. Based on the received reports, the OLT then sizes and schedules the next transmission grants to the ONUs generally in a round-robin manner and informs the ONUs with GATE messages about their upstream transmission windows.

While significant progress in the study of the design and performance aspects of EPONs has been made in recent years, a formal queuing theoretic analysis has proved elusive. Polling systems have been extensively studied with queueing theoretic methods, see e.g., [16, 17]. However, the analyzed polling models generally assume random switchover times between serving successive stations, whereby the switchover times are *independent* of the traffic generation and service. In contrast, in an EPON, the service (transmission grant) of an ONU follows immediately (separated by a guard time) after the transmission of the preceding ONU to ensure high utilization of the upstream transmission bandwidth. The switchover time is therefore generally highly *dependent* on the roundtrip delays and the masking of the roundtrip delays through upstream transmissions, significantly complicating formal analysis.

In this paper, we contribute an analysis of the mean packet delay in an EPON with gated service [18], where each ONU is granted a transmission window equal to its reported amount of upstream traffic. Our focus on gated service is motivated by recent results demonstrating that gated service provides the smallest packet delays, particularly for high loads [19]. We note that an important drawback of gated service is that an ONU with a high traffic volume can monopolize the upstream bandwidth resulting in unfair bandwidth allocation.

We consider two reporting strategies with gated service: (*i*) sending the REPORT message at the beginning of a granted upstream transmission, and (*ii*) sending the REPORT message at the end of the upstream transmission. We consider Poissonian packet generation at the ONUs with an arbitrary packet size distribution. We initially examine the special case of an EPON with a single ONU and provide an exact closed-form delay expression when sending the REPORT at the end of the transmission window, and an exact Markov chain model involving the numerical solution of a system of equations when sending the REPORT at the beginning of the upstream transmission. We note that even the special case of one ONU can not be accommodated by the existing polling models with independent switchover times since the delay between two successive upstream transmissions is (deterministically) equal to the ONU-OLT-ONU round trip propagation delay (plus very small processing delays) when sending the REPORT at the end. When sending the REPORT at the beginning, the delay between successive upstream transmissions depends on the duration of the preceding transmission and the round trip propagation delay.

For reporting at the beginning of an upstream transmission, we conduct an approximate packet delay analysis for an EPON with multiple ONUs. We verify the correctness of the exact delay analyses for a single ONU and the accuracy of the approximate delay analysis for multiple ONUs through simulations. We also identify the relative advantages of the two reporting strategies.

This paper is structured as follows. In the following subsection we review related work on the analysis of EPONs and polling systems. In Section 2, we present our EPON model and the main notations. In Section 3, we analyze the packet delay for reporting at the end of an upstream transmission, while we analyze the delay for reporting at the beginning of an upstream transmission in Section 4. In Section 5, we derive a lower bound on the packet delay for both reporting strategies. In Section 6, we validate our queueing theoretic analysis with simulations. We summarize our contributions in Section 7.

1.A. Related work

EPONs have so far mainly been evaluated through simulations which provide valuable insights into their characteristics, but need to be complemented with formal mathematical analysis for a deeper understanding. Only few existing studies have attempted to formally analyze the various aspects of EPON operation. Bhatia and Bartos [20] conduct an approximate analysis of the collision probability for the messages sent by the ONUs to the OLT for registration, i.e., when establishing the first communication between new ONUs and the OLT. The analysis provides contention window sizes for an efficient registration process. EPONs with a fixed bandwidth allocation to the ONUs have been analyzed by Holmberg [21] for regulated (e.g., Leaky Bucket shaped) input traffic and by Lannoo et al. [22] for Poisson packet traffic. These analyses show that the static bandwidth allocation can meet delay constraints only at the expense of low network utilization, motivating the use of dynamic bandwidth allocation.

In [22], Lannoo et al. have made significant progress toward a formal delay analysis for an EPON with dynamic bandwidth allocation using gated service. They have derived a Markov chain model for the cycle length in a multi-ONU EPON with reporting at the end of the upstream transmission. By numerically solving the system of equations corresponding to the Markov chain model, they obtain the mean cycle length, which is then used to approximate the mean delay. Our analysis complements and advances this analysis as follows. First, we derive an exact closed-form expression for the delay in a gated-service single-ONU EPON with reporting at the end. We also consider gated-service EPONs with reporting at the beginning of the upstream transmission, deriving a Markov chain model for the cycle length, the exact delay in a single-ONU EPON, and an approximation of the delay in a multi-ONU EPON.

Luo and Ansari [23,24] propose and analyze a dynamic bandwidth allocation scheme with traffic prediction, whereby the prediction error is assumed to be Gaussian. The average delay is expressed in terms of the Gaussian prediction error distribution. Bhatia *et al.* [25] analyze the mean transmission grant size and cycle time for reporting at the end of an upstream transmission for a single ONU and for low-load and high-load regimes for multiple ONUs. The delay that a generated packet experiences until it is reported to the OLT and the delay until the packet is transmitted in a granted transmission window, which contribute significantly to the total packet delay, as we demonstrate in this paper, are not examined in [25].

Takagi [16, 17] provides extensive overviews of the literature on the analysis of polling systems with independent switchover times. Building directly on this polling system analysis literature, Park et al. [26] consider an EPON model with random independent switchover times and derive a closed form delay expression for multiple ONUs. The EPON model with independent switchover times holds only when successive upstream transmissions are separated by a random time interval sufficiently large to "de-correlate" successive transmissions, which would significantly reduce bandwidth utilization in practice. The literature on polling systems with correlations is relatively sparse, see for instance [27–32], and considers correlations that are different from the dependencies arising in EPONs.

2. General EPON model and notations

We let C denote the upstream transmission speed (in bit/sec) of the EPON. We let O denote the number of ONUs independently generating packets according to Poisson processes with rates $\lambda_1, \lambda_2, \ldots, \lambda_O$ (packets/sec) and denote $\lambda = \sum_{o=1}^{O} \lambda_o$ for the overall packet generation rate on the EPON. We consider heterogeneous packet sizes $L^{(n)},\ n = 1, \ldots, \eta$, whereby a given generated packet has size $L^{(n)}$ (in bit) with probability α_n. We denote the mean packet size by $\bar{L} = \sum_{n=1}^{\eta} \alpha_n \cdot L^{(n)}$, the variance of the packet sizes by σ_L^2, and the traffic intensity (load) by $\rho = \lambda \bar{L}/C$, which we require to satisfy $\rho < 1$ throughout.

We decompose the packet delay into three main random components plus the transmission and propagation delay for the actual upstream transmission of the given packet. We denote

- D_1 for the time from the instant a packet is generated at the ONU to the instant when the next REPORT message is sent, notifying the OLT about the generated packet.
- D_2 for the time between sending the REPORT message notifying the OLT about the packet and the beginning of the corresponding upstream transmission at the ONU.
- D_3 for the time between the beginning of the upstream transmission containing the considered packet and the actual beginning of the transmission of the packet.
- τ for the upstream propagation delay of the considered packet.

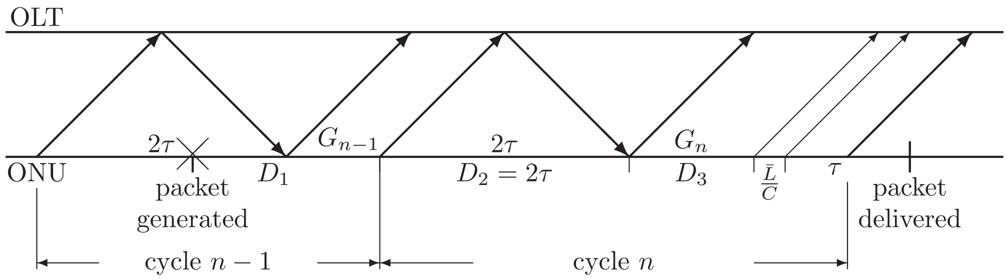

Fig. 1. Illustration of packet delay for EPON with a single ONU with reporting at the end of an upstream transmission: The generated packet experiences a delay D_1 before it is reported to the OLT with the report appended to upstream transmission grant of length G_{n-1} in cycle $n-1$. The corresponding grant for cycle n arrives at the ONU after a delay of $D_2 = 2\tau$. The packet experiences an additional delay D_3 within the grant of length G_n until its upstream transmission commences. Finally, the packet experiences its transmission delay (which has a mean of $\bar{L}/C$) and propagation delay τ.

- $\bar{L}/C$ for the mean transmission delay of the considered packet.

With these definitions we obtain the total packet delay D as

$$D = D_1 + D_2 + D_3 + \tau + \frac{\bar{L}}{C}. \tag{1}$$

In order not to obstruct our main modelling approaches, we neglect the guard time, the transmission time of the REPORT message, and the transmission time of the GATE message in our analysis. These times are relatively small compared to the propagation delay and the durations of the upstream transmissions (which typically contain several data packets) and could be incorporated into our models in a straightforward manner following the same strategies as [25] uses for modelling these delays.

3. Delay analysis for sending REPORT at end of upstream transmission

In this section we analyze the mean packet delay in an EPON with reporting at the end of the upstream transmission, as is common in the existing EPON studies, see e.g., [2, 7, 18, 22, 25]. We initially consider a single ONU, i.e., $O = 1$, that generates packet traffic at the rate $\lambda_1 = \lambda$. We discretize time and consider the time instant after transmitting one bit upstream, which takes $1/C$ (seconds). For any such bit i, let N_i be a random variable denoting the number of packets that are generated during the $1/C$ bit time period. For the considered Poisson packet generation process arrival, N_i is Poisson distributed with mean λ/C. Let $l_1, l_2, \ldots, l_{N_i}$ be random variables denoting the sizes of the generated packets. Let X_i be a random variable denoting the amount (in bit) of generated traffic during the ith bit time period, i.e.,

$$X_i = l_1 + \cdots + l_{N_i}. \tag{2}$$

Wald's Equation [33, p. 170], states that for N independent and identically distributed random variables $Y_1, Y_2, \ldots, Y_N$ that are independent of N, $\mathbb{E}[Y_1 + Y_2 + \cdots + Y_N] = \mathbb{E}Y_1\mathbb{E}N$. With Wald's Equation, $\mathbb{E}X_1 = \bar{L}\mathbb{E}N_1 = \bar{L}\lambda/C = \rho$.

Let G_n be a random variable denoting the transmission time (in seconds) of the nth grant. As illustrated in Fig. 1, the size of the nth grant is equal to the sum of the sizes of the packets newly generated during the preceding cycle, i.e., the $(n-1)$th cycle. This preceding cycle lasts $2\tau + G_{n-1}$ seconds (i.e., $(2\tau + G_{n-1})C$ bit times). Hence,

$$G_n = \frac{X_1 + \cdots + X_{(2\tau+G_{n-1})C}}{C}. \tag{3}$$

3.A. Evaluation of mean grant size $\mathbb{E}G$ and mean cycle length $\mathbb{E}Z$

Since in steady-state $\mathbb{E}G_n = \mathbb{E}G_{n-1} = \mathbb{E}G$, we derive from (3), by Wald's Equation,

$$\begin{aligned}
\mathbb{E}G &= \mathbb{E}X_1 \mathbb{E}(2\tau + \mathbb{E}G_{n-1}) && (4)\\
&= \rho(2\tau + \mathbb{E}G), && (5)
\end{aligned}$$

which gives the mean grant size of

$$\mathbb{E}G = \frac{2\tau\rho}{1-\rho}. \tag{6}$$

From this we obtain the mean cycle length $\mathbb{E}Z$ in steady-state as

$$\mathbb{E}Z = 2\tau + \frac{2\tau\rho}{1-\rho} = \frac{2\tau}{1-\rho}. \tag{7}$$

3.B. Evaluation of second moment of grant size $\mathbb{E}G^2$ and cycle length $\mathbb{E}Z^2$

Wald's Equation for the variance [33, p. 170], states that for N independent and identically distributed random variables $Y_1, Y_2, \ldots, Y_N$ that are independent of N, $\mathbb{E}(Y_1 + Y_2 + \cdots + Y_N - N\mathbb{E}Y_1)^2 = \mathbb{V}Y_1 \mathbb{E}N$, where $\mathbb{V}Y_1$ denotes the variance of Y_1. With this Wald's Equation for the variance and (3), we obtain

$$\mathbb{E}\left(G_n - (2\tau + G_{n-1})C\mathbb{E}\left(\frac{X_1}{C}\right)\right)^2 = \frac{\mathbb{V}(X_1)}{C}\,\mathbb{E}(2\tau + G_{n-1}). \tag{8}$$

From this equation we obtain the second moment of the grant size as follows. We first calculate $\mathbb{V}(X_1)$, which is (using Wald's Equation in the fourth step)

$$\begin{aligned}
\mathbb{V}(X_1) &= \mathbb{E}X_1^2 - \rho^2 && (9)\\
&= \mathbb{E}(X_1 - N_1\bar{L} + N_1\bar{L})^2 - \rho^2 && (10)\\
&= \mathbb{E}(X_1 - N_1\bar{L})^2 + 2\mathbb{E}(X_1 N_1 \bar{L}) - \mathbb{E}(N_1\bar{L})^2 - \rho^2 && (11)\\
&= \sigma_L^2 \mathbb{E}N_1 + 2\bar{L}^2\mathbb{E}N_1^2 - \bar{L}^2\mathbb{E}N_1^2 - \rho^2 && (12)\\
&= \sigma_L^2 \frac{\lambda}{C} + \bar{L}^2 \frac{\lambda}{C}\left(\frac{\lambda}{C} + 1\right) - \rho^2 && (13)\\
&= \rho\left(\frac{\sigma_L^2}{\bar{L}} + \bar{L}\right), && (14)
\end{aligned}$$

where we used when passing from (11) to (12) that

$$\begin{aligned}
\mathbb{E}(X_1 N_1) &= \sum_{k=0}^{\infty} \mathbb{P}\left[N_1 = k\right] \mathbb{E}(X_1 k | N_1 = k) && (15)\\
&= \sum_{k=0}^{\infty} k\mathbb{P}\left[N_1 = k\right] \mathbb{E}(l_1 + \ldots + l_k) && (16)\\
&= \sum_{k=0}^{\infty} k\mathbb{P}\left[N_1 = k\right] k\bar{L} && (17)\\
&= \bar{L}\mathbb{E}N_1^2. && (18)
\end{aligned}$$

The step from (12) to (13) follows by noting that a Poisson distributed random variable with mean $\mathbb{E}N_1 = \frac{\lambda}{C}$ has the second moment $\mathbb{E}N_1^2 = \frac{\lambda}{C}\left(\frac{\lambda}{C}+1\right)$ [34, p. 400]. Thus, the right-hand side of (8) equals:

$$\left(\frac{\sigma_L^2}{\bar{L}} + \bar{L}\right)\frac{2\tau\rho}{C(1-\rho)}. \tag{19}$$

On the other hand, note that in steady-state $\mathbb{E}G_n^2 = \mathbb{E}G_{n-1}^2 = \mathbb{E}G^2$. The left-hand side in (8) equals

$$\begin{aligned} & \mathbb{E}G_n^2 - 2\mathbb{E}G_n(2\tau + G_{n-1})\rho + \rho^2\mathbb{E}(2\tau + G_{n-1})^2 && (20)\\ = \; & \mathbb{E}G^2 - 4\tau\rho\mathbb{E}G - 2\rho\mathbb{E}G_nG_{n-1} + \rho^2(2\tau)^2 + 4\tau\rho^2\mathbb{E}G + \rho^2\mathbb{E}G^2. && (21)\end{aligned}$$

In order to solve (8) for $\mathbb{E}G^2$ we have to determine $\mathbb{E}G_nG_{n-1}$, which is (using again Wald's equation)

$$\begin{aligned} & \sum_{k=0}^{\infty}\mathbb{P}\left[G_{n-1}=k\right]\mathbb{E}(G_n k|G_{n-1}=k) && (22)\\ = \; & \sum_{k=0}^{\infty}\mathbb{P}\left[G_{n-1}=k\right]k\mathbb{E}\left(\frac{X_1+\ldots+X_{(2\tau+k)C}}{C}\right) && (23)\\ = \; & \sum_{k=0}^{\infty}\mathbb{P}\left[G_{n-1}=k\right]k\mathbb{E}X_1(2\tau+k) && (24)\\ = \; & \rho 2\tau\mathbb{E}G + \rho\mathbb{E}G^2. && (25)\end{aligned}$$

Therefore, the left-hand side of (8) equals

$$\begin{aligned} & \mathbb{E}G^2 - 4\tau\rho\mathbb{E}G - 2\rho(\rho 2\tau\mathbb{E}G + \rho\mathbb{E}G^2) + \rho^2(2\tau)^2 + 4\tau\rho^2\mathbb{E}G + \rho^2\mathbb{E}G^2 && (26)\\ = \; & (1-\rho^2)\mathbb{E}G^2 - 4\tau\rho\frac{2\tau\rho}{1-\rho} + \rho^2(2\tau)^2. && (27)\end{aligned}$$

Comparing this to (19) gives

$$\begin{aligned} \mathbb{E}G^2 &= \frac{1}{1-\rho^2}\left[4\tau\rho\frac{2\tau\rho}{1-\rho} - \rho^2(2\tau)^2 + \rho\left(\frac{\sigma_L^2}{\bar{L}}+\bar{L}\right)\frac{2\tau}{C(1-\rho)}\right] && (28)\\ &= \frac{2\tau\rho}{(1-\rho)(1-\rho^2)}\left[2\rho\tau + 2\tau\rho^2 + \frac{\sigma_L^2}{C\bar{L}} + \frac{\bar{L}}{C}\right]. && (29)\end{aligned}$$

From this formula we also obtain an explicit formula for the second moment of the cycle length by

$$\begin{aligned} \mathbb{E}Z^2 &= (2\tau)^2 + 2\cdot 2\tau\mathbb{E}G + \mathbb{E}G^2 && (30)\\ &= (2\tau)^2 + \frac{8\tau^2\rho}{1-\rho} + \mathbb{E}G^2 && (31)\\ &= (2\tau)^2 + \frac{8\tau^2\rho}{1-\rho} + \frac{2\tau\rho}{(1-\rho)(1-\rho^2)}\left[2\rho\tau + 2\tau\rho^2 + \frac{\sigma_L^2}{C\bar{L}} + \frac{\bar{L}}{C}\right] && (32)\\ &= \frac{2\tau}{(1-\rho)(1-\rho^2)}\left[2\tau + 2\tau\rho + \frac{\rho\sigma_L^2}{C\bar{L}} + \frac{\rho\bar{L}}{C}\right]. && (33)\end{aligned}$$

3.C. Evaluation of delay components D_1 and D_3

The mean of the first delay component D_1 corresponds to the mean residual life time of the cycle [34, p. 173] and is hence:

$$\begin{aligned} \mathbb{E}D_1 &= \frac{\mathbb{E}Z^2}{2\mathbb{E}Z} && (34)\\ &= \frac{\tau}{1-\rho} + \frac{\rho}{2(1-\rho^2)}\left(\frac{\sigma_L^2}{C\bar{L}} + \frac{\bar{L}}{C}\right). && (35)\end{aligned}$$

We obtain the mean of component D_3, i.e., the mean delay of the packet within the grant as follows. Consider an arbitrary packet that is part of the upstream transmission of cycle n. The packet was generated during cycle $n-1$, as illustrated in Fig. 1. We noted in the analysis of D_1 that the time period from the generation of the packet to the reporting at the end of cycle $n-1$ corresponds to the residual life time of the cycle. Now, we observe that the mean residual life time and the mean of the so-called backwards recurrence time coincide, see [33, Ch. 5.5]. For the considered packet, this backwards recurrence time corresponds to the time period from the beginning of cycle $n-1$ to the instant when the packet is generated. This time period has a mean of $\frac{\mathbb{E}Z^2}{2\mathbb{E}Z}$. On average, $\lambda\frac{\mathbb{E}Z^2}{2\mathbb{E}Z}$ messages (each requiring $\bar{L}/C$ upstream transmission time) are generated during this time period. These messages are transmitted upstream before the considered message. Hence

$$\begin{aligned} \mathbb{E}D_3 &= \lambda\frac{\bar{L}}{C}\frac{\mathbb{E}Z^2}{2\mathbb{E}Z} && (36) \\ &= \rho\mathbb{E}D_1. && (37) \end{aligned}$$

Inserting the components (35) and (37) into (1) we obtain for the mean packet delay

$$\begin{aligned} \mathbb{E}D &= \frac{1+\rho}{1-\rho}\tau + \frac{\rho}{2(1-\rho)}\left(\frac{\sigma_L^2}{C\bar{L}} + \frac{\bar{L}}{C}\right) + 2\tau + \frac{\bar{L}}{C} + \tau && (38) \\ &= 2\tau\frac{2-\rho}{1-\rho} + \frac{\rho}{2C(1-\rho)}\left(\frac{\sigma_L^2}{\bar{L}} + \bar{L}\right) + \frac{\bar{L}}{C}. && (39) \end{aligned}$$

4. Delay analysis for sending REPORT at beginning of upstream transmission

In this section we analyze the mean packet delay in an EPON with reporting at the beginning of an upstream transmission, as illustrated in Fig. 2. This reporting strategy is more complex to analyze than reporting at the end of the upstream transmission, since the REPORT-GATE round trip delay may or may not be masked by the upstream transmission. In the illustration in Fig. 2, the grant G_{n-2} is too short to mask the roundtrip delay; thus, the switchover time between serving the current grant G_{n-2} and the next grant G_{n-1} equals the round trip delay 2τ minus the duration of the current grant G_{n-2} plus the guard time. On the other hand, grant G_{n-1} is large enough to completely mask the roundtrip delay; thus the switchover time between serving the current grant G_{n-1} and the next grant G_n equals the guard time, which we neglect in our analysis.

The analysis of the reporting at the beginning is motivated by the shorter packet delay with this reporting strategy compared to reporting at the end of the upstream transmission. The reduction in packet delay is significant for EPONs with few ONUs, but diminishes for larger numbers of ONUs as illustrated in Section 6.

4.A. Evaluation of distribution and moments of cycle length Z

We evaluate the mean cycle length $\mathbb{E}Z$ using a Markov chain model. We let

$$\mathbf{P} := (P_{ij})_{i,j\geq 2\tau} \qquad (40)$$

denote the matrix of transition probabilities for transitioning from a cycle of length i to a cycle of length j, noting that the cycle length can be no smaller than the roundtrip propagation delay 2τ. Let Z_n be a random variable denoting the length (duration) of cycle n, i.e., $Z_n := \max(G_n,\ 2\tau)$. Note that Z_n and Z_{n-1} are independent when considering a single ONU, and that Z_n only depends on Z_{n-2}. Thus, $(Z_{2n})_{n=1}^{\infty}$ and $(Z_{2n-1})_{n=1}^{\infty}$, respectively, are Markov chains. The distribution of the even cycles $Z_{2n},\ n=1,2,\ldots$, is the same as the distribution of the odd cycles $Z_{2n+1},\ n=1,2,\ldots$. So, we may consider either one of them.

We proceed to evaluate the transition probabilities $P_{i,j}$ to pass from cycle n of length i (in units of seconds)

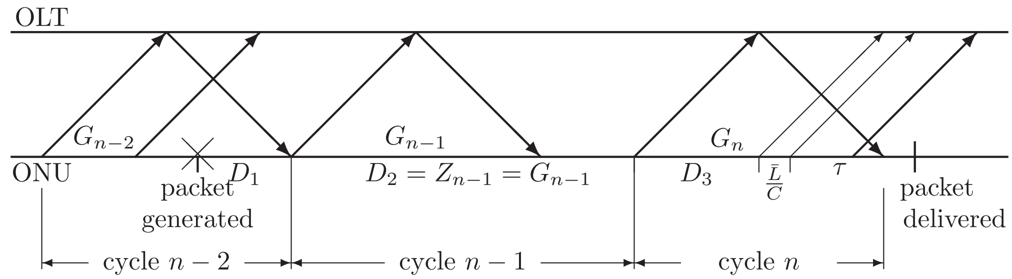

Fig. 2. Illustration of packet delay for EPON with a single ONU with reporting at the beginning of an upstream transmission: The generated packet experiences a delay D_1 before it is reported to the OLT with the report at the beginning of the upstream transmission grant of length G_{n-1} (in seconds) in cycle $n-1$. The corresponding grant for cycle n arrives at the ONU after the roundtrip delay of 2τ. In the depicted example, $G_{n-1} > 2\tau$. Thus, the length of grant $n-1$ determines the length of cycle $n-1$ and the delay component D_2. In addition, the packet experiences the delay D_3 within the upstream transmission grant n, the transmission delay (with mean $\bar{L}/C$) and the propagation delay τ.

to a cycle $n+2$ of length j (in units of seconds). We obtain for $i \geq 2\tau$ and $j = 2\tau$,

$$P_{i,2\tau} = \sum_{m=0}^{\infty} \frac{(\lambda i)^m}{m!} e^{-\lambda i} \cdot q_{m,2\tau} \tag{41}$$

with

$$\begin{aligned} q_{m,2\tau} &= \mathbb{P}(m \text{ generated messages have length} \leq 2\tau\ ) & (42)\\ &= \sum_{n_1=1}^{\eta} \cdots \sum_{n_m=1}^{\eta} \alpha_{n_1} \cdots \alpha_{n_m} \mathbb{1}_{\{\frac{L^{(n_1)}}{C} + \cdots + \frac{L^{(n_m)}}{C} \leq 2\tau\}}, \qquad m \geq 0. & (43) \end{aligned}$$

Note that we do not need to sum up to $m = \infty$ in (41), since the $q_{m,2\tau} = 0$ for $m > 2\tau/(\min_n L^{(n)}/C)$. Note furthermore that (43), although mathematically explicit, is not suitable for numerical evaluation since its computational complexity is of order 2^m. For the special case of a single packet size $L^{(1)}$, (43) reduces to

$$q_{m,2\tau} = \begin{cases} 1 & \text{for } m \leq \frac{2\tau}{L^{(1)}/C} \\ 0 & \text{for } m > \frac{2\tau}{L^{(1)}/C}. \end{cases} \tag{44}$$

For the special case of a bimodal distribution, i.e., $\eta = 2$, we obtain:

$$\begin{aligned} q_{m,2\tau} &= \mathbb{P}(m \text{ generated messages have length} \leq 2\tau\ ) & (45)\\ &= \sum_{m'=0}^{m} \mathbb{P}\left(m \text{ gen. msgs. have length} \leq 2\tau \text{ and exactly } m' \text{ have length } L^{(1)}\right) & (46)\\ &= \sum_{m'=0}^{m} \mathbb{1}_{\{m'L^{(1)}+(m-m')L^{(2)} \leq 2\tau C\}} \mathbb{P}\left(\text{exactly } m' \text{ gen. msgs. have length } L^{(1)}\right) & (47)\\ &= \sum_{m'=0}^{m} \mathbb{1}_{\{m'L^{(1)}+(m-m')L^{(2)} \leq 2\tau C\}} \binom{m}{m'} \alpha_1^{m'} \cdot \alpha_2^{m-m'}, \qquad m \geq 0. & (48) \end{aligned}$$

Similarly, we obtain for the special case of a trimodal distribution, i.e., $\eta = 3$, for $m \geq 0$:

$$q_{m,2\tau} = \sum_{m_1=0}^{m} \sum_{m_2=0}^{m-m_1} \mathbb{1}_{\{m_1 L^{(1)}+m_2 L^{(2)}+(m-m_1-m_2)L^{(3)} \leq 2\tau C\}} \binom{m}{m_1} \binom{m-m_1}{m_2} \alpha_1^{m_1} \alpha_2^{m_2} \alpha_3^{m-m_1-m_2}. \tag{49}$$

Analogous formulas suitable for fast numerical evaluation can be obtained for other concrete length distributions.

We obtain similarly for $i \geq 2\tau$ and $j > 2\tau$,

$$P_{i,j} = \sum_{m=0}^{\infty} \frac{(\lambda i)^m}{m!} e^{-\lambda i} \cdot q_{m,j}, \qquad i \geq 2\tau \tag{50}$$

with

$$\begin{aligned} q_{m,j} &= \mathbb{P}\left(m \text{ generated messages have length } j\ \right) & (51)\\ &= \sum_{n_1=1}^{\eta} \cdots \sum_{n_m=1}^{\eta} \alpha_{n_1} \cdots \alpha_{n_m} \mathbb{1}_{\{\frac{L^{(n_1)}}{C} + \cdots + \frac{L^{(n_m)}}{C} = j\}}, \qquad m \geq 0, j > 2\tau. & (52)\end{aligned}$$

Note furthermore that $q_{m,j} = 0$ for $m > j/(\min_n L^{(n)}/C)$, which makes the summation in (50) finite. Also, $q_{m,j} = 0$ for $m < j/(\max_n L^{(n)}/C)$. For the special case of a single packet size $L^{(1)}$, (52) gives

$$q_{m,j} = \begin{cases} 1 & \text{for } m = \frac{j}{L^{(1)}/C} \\ 0 & \text{for } m \neq \frac{j}{L^{(1)}/C} \end{cases} \qquad m \geq 0, j > 2\tau. \tag{53}$$

For the special case of a bimodal distribution,

$$\begin{aligned} q_{m,j} &= \mathbb{P}\left(m \text{ generated messages have length } j\ \right) & (54)\\ &= \sum_{m'=0}^{m} \mathbb{P}\left(m \text{ gen. msgs. have length } j \text{ and exactly } m' \text{ have length } L^{(1)}\right) & (55)\\ &= \sum_{m'=0}^{m} \mathbb{1}_{\{m'L^{(1)}+(m-m')L^{(2)}=jC\}} \mathbb{P}\left(\text{exactly } m' \text{ gen. msgs. have length } L^{(1)}\right) & (56)\\ &= \sum_{m'=0}^{m} \mathbb{1}_{\{m'L^{(1)}+(m-m')L^{(2)}=jC\}} \binom{m}{m'} \alpha_1^{m'} \cdot \alpha_2^{m-m'}, \qquad m \geq 0, j > 2\tau. & (57)\end{aligned}$$

For the special case of a trimodal distribution, for $m \geq 0$, $j > 2\tau$:

$$q_{m,j} = \sum_{m_1=0}^{m} \sum_{m_2=0}^{m-m_1} \mathbb{1}_{\{m_1 L^{(1)}+m_2 L^{(2)}+(m-m_1-m_2)L^{(3)}=jC\}} \binom{m}{m_1} \binom{m-m_1}{m_2} \alpha_1^{m_1} \alpha_2^{m_2} \alpha_3^{m-m_1-m_2}. \tag{58}$$

With these transition probabilities $(P_{i,j})_{i,j \geq 2\tau}$ we solve the system of equations

$$\begin{pmatrix} \kappa_{2\tau} \\ \kappa_{2\tau+1} \\ \vdots \\ \kappa_K \end{pmatrix} = \begin{pmatrix} P_{2\tau,2\tau} & \cdots & P_{K,2\tau} \\ P_{2\tau,2\tau+1} & \cdots & P_{K,2\tau+1} \\ \vdots & & \vdots \\ P_{2\tau,K} & \cdots & P_{K,K} \end{pmatrix} \cdot \begin{pmatrix} \kappa_{2\tau} \\ \kappa_{2\tau+1} \\ \vdots \\ \kappa_K \end{pmatrix}, \tag{59}$$

for a K as large as possible. Noting that the typical cycle length in steady-state for a single ONU when sending the report at the end is longer than when sending the REPORT at the beginning, we obtain with the Markov-Chebyshev Inequality,

$$\mathbb{P}\left(Z_{\text{single ONU, BEG}} > K\right) \leq \mathbb{P}\left(Z_{\text{single ONU, END}} > K\right) \leq \frac{\mathbb{E}Z^2_{\text{single ONU, END}}}{K^2}. \tag{60}$$

Requiring that $\frac{\mathbb{E}Z^2_{\text{single ONU, END}}}{K^2} < \epsilon$, for, say $\epsilon = 0.05$, so as to capture $1 - \epsilon$ percent of the possible cycle lengths, we obtain

$$K \geq \sqrt{\frac{1}{\epsilon} \mathbb{E}Z^2_{\text{single ONU, END}}} \tag{61}$$

with $\mathbb{E}Z^2_{\text{single ONU, END}}$ explicitly given in (30) as a guideline for setting K. Recall that the resulting sequence $(\kappa_n)_{n=2\tau}^{K}$ is required to be a probability distribution, i.e. $\sum_{k=2\tau}^{K} \kappa_k = 1$.

From the steady state probabilities of the cycle length $(\kappa_k)_{k=2\tau}^{K}$ we obtain the mean cycle length as

$$\mathbb{E}Z = \sum_{k=2\tau}^{K} k \cdot \kappa_k, \tag{62}$$

and the second moment of the cycle length as

$$\mathbb{E}Z^2 = \sum_{k=2\tau}^{K} k^2 \cdot \kappa_k. \tag{63}$$

4.B. Evaluation of delay components for single ONU

The first delay component corresponds to the residual life of the cycle [34, p. 173] and its mean is hence given by

$$\mathbb{E}D_1 = \frac{\mathbb{E}Z^2}{2\mathbb{E}Z}. \tag{64}$$

The second delay component corresponds to the cycle length and its mean is therefore $\mathbb{E}D_2 = \mathbb{E}Z$. With reasoning analogous to Section 3.C we obtain the mean of the third delay component

$$\begin{aligned} \mathbb{E}D_3 &= \rho\mathbb{E}D_1 && (65)\\ &= \frac{\rho\mathbb{E}Z^2}{2\mathbb{E}Z}. && (66) \end{aligned}$$

Inserting in (1) and simplifying gives the mean packet delay

$$\mathbb{E}D = \frac{(1+\rho)\mathbb{E}Z^2}{2\mathbb{E}Z} + \mathbb{E}Z + \frac{\bar{L}}{C} + \tau. \tag{67}$$

Let us briefly contrast our Markov chain analysis for reporting at the beginning of an upstream transmission with the Markov chain analysis of Lannoo et al. [22] for reporting at the end. Our analysis captures the exact dynamics for a single ONU. In contrast, [22] aggregates the traffic generated by all ONUs in a multi-ONU EPON and captures the approximate dynamics for the aggregate traffic (distinguishing low and high traffic regimes).

4.C. Extension to multiple ONUs

In this section we extend the analysis for one ONU generating packets at the rate λ (packets/second) and corresponding traffic load $\rho = \lambda\bar{L}/C$ to O ONUs at the same propagation distance from the OLT generating packets at the rates $\lambda_1, \ldots, \lambda_O$, and corresponding traffic loads $\rho_o = \lambda_o\bar{L}/C,\ o = 1, \ldots, O$. We approximate the cycle length distribution for the EPON with O ONUs by the cycle length distribution of an EPON with a single ONU generating packets at the rate $\lambda = \sum_{o=1}^{O} \lambda_o$. Thus, D_1 and D_2 for O ONUs are approximated by the respective quantities for a single ONU.

To approximate the third delay component D_3, we consider the delay D_3^o experienced by a packet of ONU o as it is waiting from the beginning of the upstream transmission containing the packet to the actual beginning of the transmission of the packet at ONU o. Following (37), we obtain the approximation

$$\mathbb{E}D_3^o = \rho_o\mathbb{E}D_1. \tag{68}$$

We then obtain an approximation of the mean of the third delay component as a convex combination of the delays of the O ONUs:

$$\begin{aligned}
\mathbb{E}D_3 &= \sum_{o=1}^{O} \frac{\lambda_o}{\sum_{q=1}^{O} \lambda_q} \mathbb{E}D_3^o &(69)\\
&= \frac{\mathbb{E}D_1}{\rho} \sum_{o=1}^{O} \rho_o^2. &(70)
\end{aligned}$$

The motivation for this formula is as follows. Since on average a fraction of $\lambda_o / \sum_{q=1}^{O} \lambda_q$ of the traffic is generated by ONU o, the delay experienced in the third component for this fraction of traffic corresponds to $\mathbb{E}D_3^o$. Thus, the third delay component is the weighted sum of the delays of the O ONUs.

We note that an analogous extension of the closed-form analysis for reporting at the end of an upstream transmission from Section 3 to multiple ONUs does not give accurate results. This is mainly due to the delay component D_2, which is equal to 2τ when considering a single ONU reporting at the end. With multiple ONUs reporting at the end, the delay component D_2 may grow larger than 2τ depending on the upstream traffic volume of the other ONUs, thus increasing the expected cycle length $\mathbb{E}Z$, which in turn influences the delay components D_1 and D_3. We leave the analysis of these dependencies for future research. We also remark that verifying simulations in Section 6 demonstrate for EPONs with a moderate to large number of ONUs that the above extension for reporting at the beginning quite accurately characterizes the mean delays for reporting at the end, i.e., that both reporting strategies give the same mean delays for EPONs with a moderate to large number of ONUs.

5. M/G/1 approximation for EPON with small propagation delay

In this section we consider an EPON with a propagation delay that tends to zero and derive a lower bound on the expected packet delay that applies to both reporting strategies. Letting the propagation delay in an EPON tend to zero, we observe that each generated packet could be instantaneously reported to the OLT, which could in turn instantaneously give the grant for the upstream transmission of the packet. The delay experienced by the packet from its generation to its complete delivery to the OLT would then consist of the queueing delay at the ONU as well as the upstream transmission (and propagation) delay. With the considered Poissonian packet generation with rate λ (packets/second) at the ONU in conjunction with the arbitrary packet size distribution with mean $\bar{L}$ (bit /packet) and variance σ_L^2 and the fixed upstream transmission rate C (bit/second) and corresponding load $\rho = \lambda \bar{L}/C$, the queueing at the ONU would correspond to the queuing in an M/G/1 model. According to the Pollaczek-Khinchine formula [34] the mean queueing delay in the ONU would thus be given by:

$$\mathbb{E}D_{\mathrm{M/G/1}} = \frac{\lambda(\frac{\sigma_L^2}{C^2} + \frac{\bar{L}^2}{C^2})}{2(1-\rho)}, \tag{71}$$

which simplifies for the case of a single packet size $L^{(1)}$ to

$$\mathbb{E}D_{\mathrm{M/G/1}} = \frac{\rho L^{(1)}}{2C(1-\rho)}. \tag{72}$$

We obtain a lower bound on the expected packet delay in an EPON with propagation delay $\tau > 0$ by considering the following two points:

(A) In addition to the queueing delay, a packet experiences three times the propagation delay [(i) for reporting to the OLT, (ii) for receiving the grant from the OLT, and (iii) for the upstream propagation of the packet] and the upstream transmission delay.

Table 1. Default parameters for numerical analysis.

Description	Symbol	Default value
Number of ONUs	O	10
Fiber length	ℓ	9.6 km
Data rate	C	1 Gb/s
Packet size	L	1500 byte
Signal propagation speed	$2c_0/3$	200000 km/s
Max. considered cycle length	K	128 packets

(B) The average packet delay is at least four times the propagation delay. To see this note that the cycle duration is at least twice the propagation delay, thus resulting in an average delay of at least the propagation delay until a packet is reported. In addition, three propagation delays are accrued for the REPORT, GATE, and upstream transmission as outlined in (A).

Thus, we obtain the lower bound for the mean packet delay:

$$\mathbb{E}D \geq \max\left(4\tau,\ 3\tau + \frac{\rho}{2C(1-\rho)}\left(\frac{\sigma_L^2}{\bar{L}} + \bar{L}\right) + \frac{\bar{L}}{C}\right). \tag{73}$$

It is interesting to compare this lower bound with the exact mean delay for reporting at the end of the upstream transmission as derived in (38). Clearly, both this exact mean delay and the lower bound coincide for small propagation delays τ, or for small loads ρ. In addition, we expect a fairly accurate characterization of the packet delay through the lower bound when the queueing delay dominates the overall packet delay. We remark that analyzing the EPON within the framework of multiaccess reservation systems [35, Section 4.5.1] gives approximations that are similar to the derived lower bound.

6. Numerical evaluation

In this section, we evaluate the delay performance of the EPON with gated service using our analytical models and verifying discrete event simulations. We evaluate the *mean packet delay* $\mathbb{E}D$ as a function of the traffic load $\rho = \lambda\bar{L}/C$. For convenience we express the mean packet delay in multiples of the propagation delay τ. Each ONU generates the same amount of traffic according to a Poisson process with intensity $\lambda = (\rho C/\bar{L})/O$. The traffic load $\rho, 0 \leq \rho \leq 1$ is the total amount of traffic generated by all ONUs, normalized by the data rate C. All buffers are assumed to be of infinite size. Therefore, the offered load ρ can also be interpreted as the mean aggregate throughput of the EPON in steady state.

The different system parameters and their default values are summarized in Table 1. Note that with these default parameter settings, the transmission delay of a packet corresponds to one quarter of the propagation delay, i.e., $L/C = \ell/[4(2c_o/3)] = \tau/4$. Simulation results are calculated from the performance results for each individual packet according to the method of batch-means with a simulation duration of 10^6 packet receptions where the first 10^5 receptions are used as warm-up phase and the remaining packets are divided into 100 batches. Confidence intervals are shown for the mean delay for a confidence level of 95%.

6.A. *Single ONU*

Fig. 3 shows the throughput-delay performance for the special case of only a single ONU being attached to the OLT. Results are shown for both reporting at the beginning and at the end of an upstream transmission.

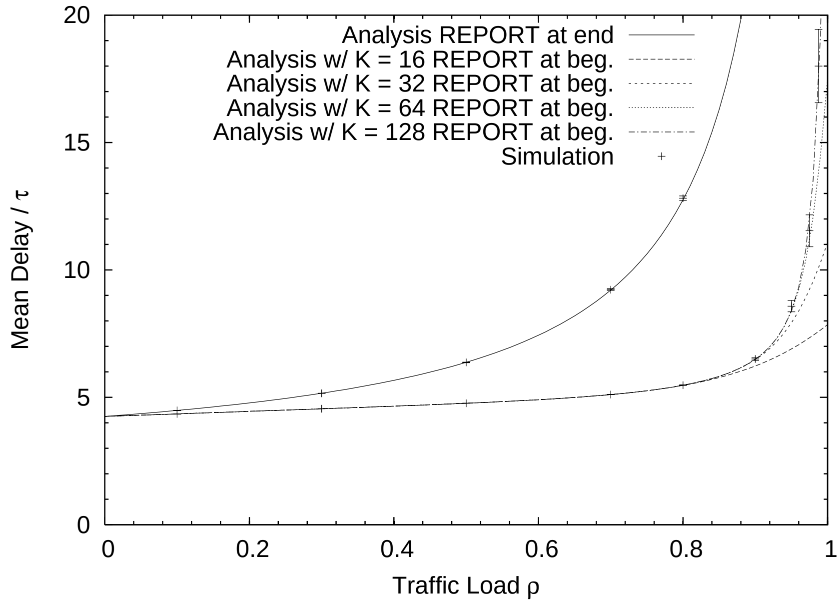

Fig. 3. Mean delay vs. mean aggregate throughput for a single ONU. The analytical delay results for reporting at the *beginning* of an upstream transmission are plotted for different maximally considered cycle lengths K.

In the former case it is important to determine an appropriate maximum considered cycle length K for the numerical evaluation of the analytic formulae. For small K, the precision of the analytical model degrades. On the other hand, for large K, the computational effort of the numerical evaluation increases. The results for different values of K illustrate that a value of $K = 128$ is sufficiently large to match simulation and analysis close enough that there is no visible deviation between analysis and simulation. Therefore, we use $K = 128$ as default parameter for the following investigations. There is no deviation between the analytical model and the simulation for reporting at the end of an upstream transmission. This is to be expected because both analytical models are exact for the single ONU case. For low traffic loads the delay is slightly larger than twice the roundtrip propagation delay, i.e., 4τ, which is the expected lower bound according to the analysis. The delay is slightly larger than 4τ due to the time required to transmit the packet which is $L/C = \tau/4$.

Reporting at the end of an upstream transmission results in gaps between successive upstream transmissions when only a single ONU is active because the ONU has to remain idle after sending a REPORT message until the corresponding GATE message arrives. As the load increases and the grants issued by the OLT get longer, the bandwidth wasted due to these gaps gets smaller relative to the amount of data sent by the ONU. However, the numerical results show that reporting at the beginning of an upstream transmission results in a clear performance advantage. In this case the network can be utilized by up to 75% of its capacity without significantly increasing the delay as opposed to a continuously increasing delay when reporting at the end of an upstream transmission. We observe that this performance difference is very pronounced in the single ONU case. As the number of ONUs increases, the idle gap of one ONU will more likely be used for sending data by other ONUs.

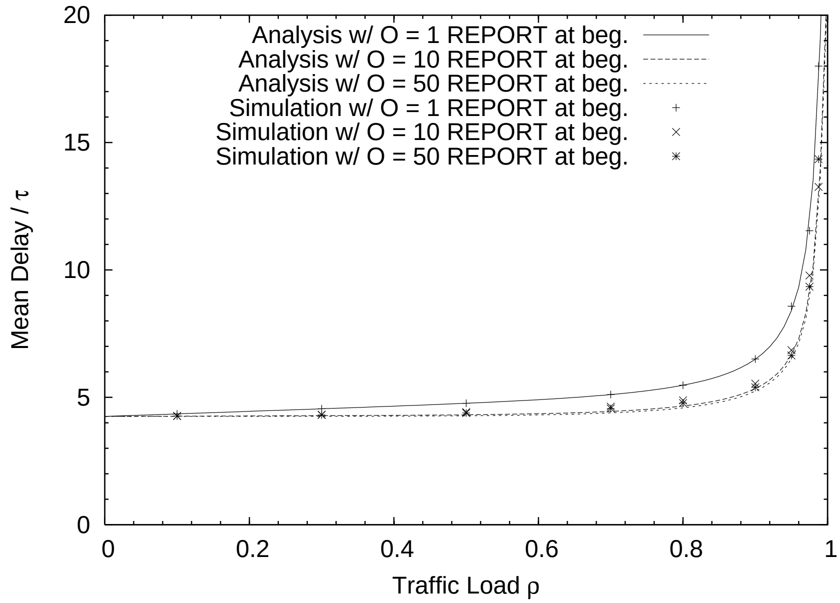

Fig. 4. Mean delay vs. mean aggregate throughput for different numbers of ONUs O and reporting at the *beginning* of an upstream transmission.

6.B. Different numbers of ONUs

In Figs. 4 and 5 we examine the delay performance for different numbers O of ONUs attached to the same OLT. (To be able to distinguish between the simulation results for different numbers of ONUs O, no confidence intervals are shown in these plots and different point styles are used instead. For $O = 1$ and $O = 10$ the confidence intervals are shown in Fig. 3 and 6.) For reporting at the beginning of an upstream transmission, Fig. 4 shows that the delay decreases slightly with increasing number of ONUs. This is due to the fact that the traffic load is distributed among more ONUs, resulting in shorter cycles and smaller grants and thus less queuing at the ONUs. We note that with a larger number of ONUs, more guard times are required to separate the different upstream transmissions, thus increasing the delay. As noted in Section 2, our model ignores guard times, which could be accommodated in a straightforward manner.

In Fig. 5, *simulation* results are shown for different numbers of ONUs and reporting at the *end* of an upstream transmission. Note, however, that the *analytical* results are shown for reporting at the *beginning* of an upstream transmission (except for $O = 1$). In other words, the analytical curves for $O = 10$ and $O = 50$ in Fig. 5 are the same as in Fig. 4. Comparing both figures illustrates that the throughput-delay performance for reporting at the end of an upstream transmission converges towards that of reporting at the beginning as the number of ONUs O increases. Overall, for systems with 10 or more ONUs, which should be the majority of all practical systems, the delay is close to the theoretical lower bound of 4τ and does not increase significantly up to a traffic load of 75% of the network capacity in both cases. We use $O = 10$ as the default value in our investigations below.

6.C. Different fiber lengths

Fig. 6 shows the impact of the fiber length ℓ between the ONUs and the OLT for reporting at the beginning of an upstream transmission. We do not consider reporting at the end of an upstream transmission separately

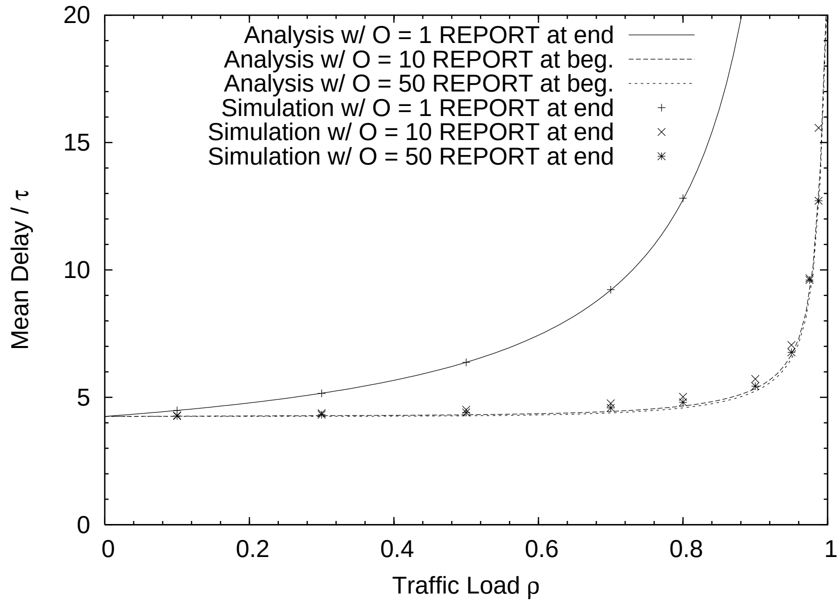

Fig. 5. Mean delay vs. mean aggregate throughput for different numbers of ONUs O and reporting at the *end* of an upstream transmission.

because the results would be almost the same for the reasons discussed in the previous section. The delay depicted in Fig. 6 is given in multiples of propagation delay τ of the system with $\ell = 9.6$ km fiber length in all three cases. Simulation and analytical results match well. Note that the effect from changing the fiber length is mostly limited to an up or down shift of the delay curve while the shape of the curve remains largely the same. The M/G/1 model of Section 5, which is exact for the special case of $\ell = 0$, provides a relatively good approximation for $\ell = 4.8$ km.

6.D. Packet size distribution

In [36] it has been observed that Internet packet sizes approximately follow a bimodal distribution. In Fig. 7 we investigate the impact of such a bimodal packet size distribution on the network performance compared to the single, constant packet size of $L = 1500$ byte used before. We assume that 2/3 of all packets have a size of 50 byte and 1/3 of all packets have a size of 1500 byte to approximate the distribution measured in [36]. (To model the new packet sizes we refine the granularity of the analytical model by a factor of 30 so that one length unit in the analysis now corresponds to 50 byte as opposed to 1500 byte as before. Consequently, a 1500 byte packet now has a transmission time of 30 time units and the propagation delay corresponding to a fiber length of 9.6 km is now $\tau = 120$ time units instead of $\tau = 4$ time units. We increase the maximum considered cycle length for the analysis by a factor of 10 to $K = 1280$.)

For a single ONU, the analytical results match the simulation results very well and there is no visible deviation between the two. Note that for $O = 1$ the analytical models are not only exact for a single packet size, as observed in Fig. 3, but also for an arbitrary packet size distribution. (However, the model for sending the REPORT message at the beginning of the upstream transmission is only exact for $K \to \infty$.) For $O = 10$ ONUs the analysis still provides relatively good results.

The most important observation from this figure is that the more realistic bimodal packet size distribution

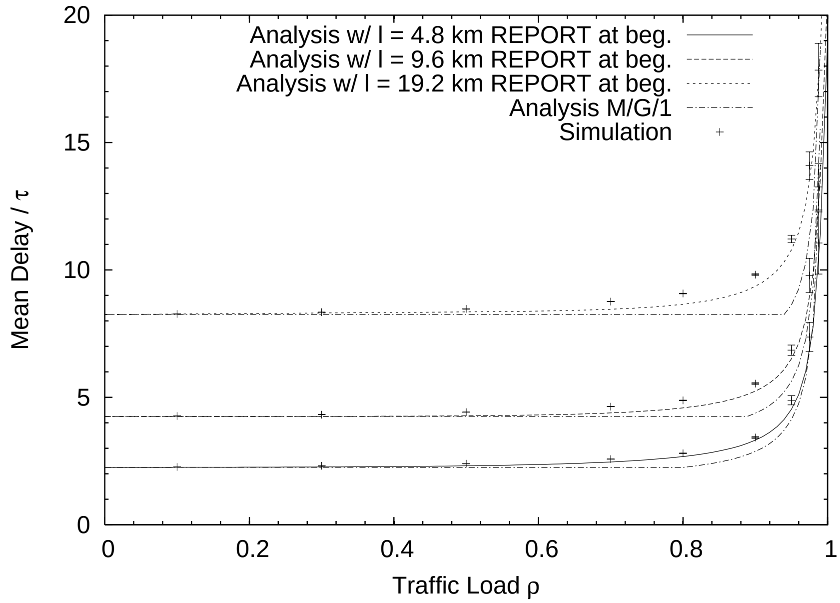

Fig. 6. Mean delay vs. mean aggregate throughput for a different fiber lengths ℓ and reporting at the *beginning* of an upstream transmission.

has only very little impact on the throughput-delay performance of the system. This is an indicator for the system performance being relatively independent of the packet size distribution in general which is an advantage for network operators since the traffic characteristics can change over time as new Internet services and applications emerge.

7. Conclusion

We have conducted a queueing theoretic analysis of the mean packet delay in an Ethernet passive optical network (EPON), a high-speed access network. We considered the basic service policy, where the granted upstream transmissions are equal to the requested upstream transmission windows, which is commonly referred to as gated service [19]. We provided exact analyses of the mean packet delay for the special case of an EPON with a single ONU, and approximated the mean packet delay in an EPON with multiple ONUs. Our extensive simulations verified the correctness of our exact analyses and the high level of accuracy achieved by our approximate analysis.

Our investigations revealed that reporting at the beginning of an upstream transmission results in significantly lower delays than appending the REPORT at the end of an upstream transmission for EPONs with a very small numbers of ONUs. For a moderate to large number of (on the order of ten) ONUs, both reporting strategies give the same mean delay. As a result, our approximate analysis for multiple ONUs reporting at the beginning applies also to EPONs with a moderate to large number of ONUs reporting at the end of an upstream transmission. From a practical perspective, our results show that the investigated EPON protocols allow the network operator to utilize the network up to 75% without significantly increasing the delay experienced by the users above the minimum mean packet delay of four times the one-way propagation delay. Also, our results indicate that the delay performance is relatively independent of the packet size distribution, which contributes to the future-proofness of the system.

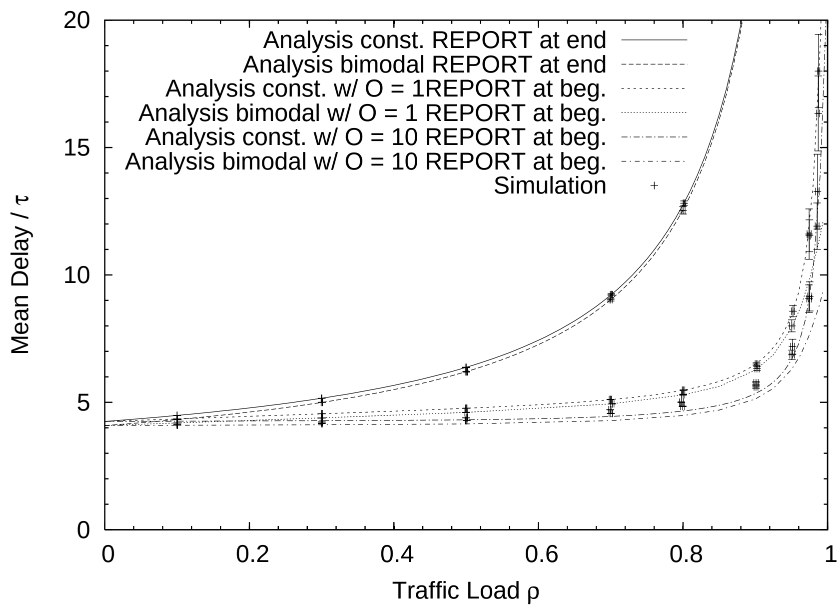

Fig. 7. Mean delay vs. mean aggregate throughput for a bimodal vs. the constant packet size distribution.

Future research avenues include the exact delay analysis of other QoS supporting service policies such as limited service. Limited service poses interesting analytical challenges, as it can be viewed as a mixture of the gated service analyzed in this paper and the so-called fixed service discipline (analyzed in [21], though from a different perspective). One the one hand, one would expect cycles similar to the gated service, but one additionally would have to consider the data that is queued up in case it cannot be sent due to reaching the transmission limit.

Acknowledgments

This work was supported by the DFG Research Center MATHEON "Mathematics for key technologies" in Berlin. We are grateful to Dr. Michael McGarry of ADTRAN Inc., formerly with Arizona State University, for in-depth discussions on EPONs.

References

1. F. An, K. Kim, D. Gutierrez, S. Yam, E. Hu, K. Shrikhande, and L. Kazovsky, "SUCCESS: a next-generation hybrid WDM/TDM optical access network architecture," J. Lightwave Technol. **22**, 2557–2569 (2004).
2. C. Assi, Y. Ye, S. Dixit, and M. Ali, "Dynamic bandwidth allocation for Quality-of-Service over Ethernet PONs," IEEE J. Sel. Area Comm. **21**, 1467–1477 (2003).
3. X. Bai, A. Shami, and C. Assi, "Statistical bandwidth multiplexing in Ethernet passive optical networks," in *Proc. of IEEE GLOBECOM*, vol. 4, pp. 1920–1924 (2005).
4. A. Banerjee, Y. Park, F. Clarke, H. Song, S. Yang, G. Kramer, K. Kim, and B. Mukherjee, "Wavelength-division-multiplexed passive optical network (WDM-PON) technologies for broadband access: a review," J. Opt. Netw. **4**, 737–758 (2005).

5. C. Foh, L. Andrew, E. Wong, and M. Zukerman, “FULL-RCMA: a high utilization EPON,” IEEE J. Sel. Area Comm. **22**, 1514–1524 (2004).
6. M. Hajduczenia, H. da Silva, and P. Monteiro, “On efficiency of Ethernet passive optical networks (EPONs),” in *Proc. of IEEE Int. Symposium on Computers and Communications (ISCC)*, pp. 566–571 (2006).
7. G. Kramer, B. Mukherjee, and G. Pesavento, “Ethernet PON (ePON): design and analysis of an optical access network,” Photonic Netw. Commun. **3**, 307–319 (2001).
8. K. Kwong, D. Harle, and I. Andonovic, “Dynamic bandwidth allocation algorithm for differentiated services over WDM EPONs,” in *Proc. of The Ninth International Conference on Communications Systems*, pp. 116–120 (2004).
9. M. Ma, Y. Zhu, and T. Cheng, “A bandwidth guaranteed polling MAC protocol for Ethernet passive optical networks,” in *Proc. of IEEE INFOCOM*, vol. 1, pp. 22–31 (2003). San Francisco, CA.
10. R. Mastrodonato and G. Paltenghi, “Analysis of a bandwidth allocation protocol for Ethernet passive optical networks (EPONs),” in *Proc. of IEEE Int. Conf. on Transparent Optical Networks*, pp. 241–244 (2005).
11. M. McGarry, M. Maier, and M. Reisslein, “Ethernet PONs: a survey of dynamic bandwidth allocation (DBA) algorithms,” IEEE Commun. Mag. **42**(8), S8–S15 (2004).
12. H. Naser and H. Mouftah, “A joint-ONU interval-based dynamic scheduling algorithm for Ethernet passive optical networks,” IEEE ACM T. Network. **14**, 889–899 (2006).
13. A. Shami, X. Bai, C. Assi, and N. Ghani, “Jitter Performance in Ethernet Passive Optical Networks,” J. Lightwave Technol. **23**, 1745–1753 (2005).
14. A. Sierra and S. V. Kartalopoulos, “Evaluation of two prevalent EPON networks using simulation methods,” in *Proc. of the Advanced Int. Conf. on Telecommunications and Int. Conf. on Internet and Web Applications and Services*, pp. 48–53 (2006).
15. C. Xiao, B. Bing, and G. Chang, “An efficient MAC protocol with pre-allocation for high-speed WDM passive optical networks,” in *Proc. of IEEE Infocom*, pp. 444-454 (2005).
16. H. Takagi, *Analysis of Polling Systems* (MIT Press, 1986).
17. H. Takagi, “Analysis and application of polling models,” in *Performance Evaluation: Origins and Directions, Lecture Notes in Computer Science, Vol. 1769*, G. Haring, C. Lindemann, and M. Reiser, eds., pp. 423–442 (Springer, 2000).
18. G. Kramer, B. Mukherjee, and G. Pesavento, “IPACT: A dynamic protocol for an Ethernet PON (EPON),” IEEE Commun. Mag. **40**(2), 74–80 (2002).
19. G. Kramer, *Ethernet Passive Optical Networks* (McGraw-Hill, 2005).
20. S. Bhatia and R. Bartos, “Closed-form expression for the collision probability in the IEEE Ethernet passive optical network registration scheme,” J. Opt. Netw. **5**, 1–14 (2005).
21. T. Holmberg, “Analysis of EPONs under the static priority g scheduling scheme with fixed transmission times,” in *Proc. of IEEE Conference on Next Generation Internet Design and Engineering (NGI)*, pp. 192–199 (2006).
22. B. Lannoo, L. Verslegers, D. Colle, M. Pickavet, M. Gagnaire, and P. Demeester, “Analytical model for the IPACT dynamic bandwidth allocation algorithm in EPONs,” J. Opt. Netw. **6**, 677–688 (2007).
23. Y. Luo and N. Ansari, “Bandwidth management and delay control over EPONs,” in *Proc. of IEEE Workshop on High Performance Switching and Routing (HPSR)*, pp. 457–461 (2005).
24. Y. Luo and N. Ansari, “Dynamic upstream bandwidth allocation over Ethernet PONs,” in *Proc. of IEEE ICC*, pp. 1853–1857 (2005).

25. S. Bhatia, D. Garbuzov, and R. Bartos, "Analysis of the gated IPACT scheme for EPONs," in *Proc. of IEEE ICC*, pp. 2693–2698 (2006).
26. C. G. Park, D. H. Han, and K. W. Rim, "Packet delay analysis of symmetric gated polling system for DBA scheme in an EPON," Telecommun. Syst. **30**, 13–34 (2005).
27. I. Eliazar, "Gated polling systems with Levy inflow and inter-dependent switchover times: a dynamical-systems approach," Queuing Syst. **49**, 49–72 (2005).
28. I. Eliazar, "From polling to snowplowing," Queuing Syst. **51**, 115–133 (2005).
29. R. Groenevelt and E. Altman, "Analysis of alternating-priority queueing models with (cross) correlated switchover times," Queuing Syst. **51**, 199–247 (2005).
30. H. Levy and M. Sidi, "Polling systems with correlated arrivals," in *Proc. of IEEE Infocom*, pp. 907–913 (1989).
31. T. Lee and J. Sunjaya, "Exact analysis of asymmetric random polling systems with single buffers and correlated input process," Queuing Syst. **23**, 131–156 (1996).
32. M. M. Srinivasan, S.-C. Niu, and R. B. Cooper, "Relating polling models with zero and nonzero switchover times," Queuing Syst. **19**, 149–168 (1995).
33. D. P. Heyman and M. J. Sobel, *Stochastic Models in Operations Research: Volume I: Stochastic Processes and Operating Characteristics* (Courier Dover, 2003).
34. L. Kleinrock, *Queueing Systems: Volume I: Theory* (Wiley, 1975).
35. D. Bertsekas and R. Gallager, *Data Networks*, 2nd ed. (Prentice Hall, 1991).
36. R. Sinha, C. Papadopoulos, and J. Heidemann, "Internet Packet Size Distributions: Some Observations," (2005). URL `http://netweb.usc.edu/~rsinha/pkt-sizes/`.